

1 **Epigenetic regulation of unique genes and repetitive elements by the** 2 **KRAB zinc finger protein ZFP57**

4 **Authors:**

5 Hui Shi[†], Ruslan Strogantsev[†], Nozomi Takahashi, Anastasiya Kazachenka, Matthew C. Lorincz,
6 Myriam Hemberger and Anne C. Ferguson-Smith

8 [†]These authors contributed equally to this work.

9 **Abstract**

10 **Background:** KRAB-zinc finger proteins (KZFPs) represent one of the largest families of DNA
11 binding proteins in vertebrate genomes and appear to have evolved to silence transposable
12 elements (TEs) including endogenous retroviruses through sequence-specific targeting of
13 repressive chromatin states. ZFP57 is required to maintain the post-fertilization DNA methylation
14 memory of parental-origin at genomic imprints along with ZFP445 which is specific for imprints.
15 However, ZFP57 has multiple methylated genomic targets. Here we conduct RNA-seq and ChIP-
16 seq analyses in normal and ZFP57 mutant mouse ES cells to understand the relative importance of
17 ZFP57 at unique and repetitive regions of the genome.

18 **Results:** Over 80% of ZFP57 targets are TEs, however, ZFP57 is not essential for their repression.
19 The remaining targets lie within unique imprinted and non-imprinted sequences. Though loss of
20 ZFP57 influences imprinted genes as expected, the majority of unique gene targets lose H3K9me3
21 with little effect on DNA methylation and very few exhibiting alterations in expression. Comparison
22 with DNA methyltransferase-deleted ES cells (TKO) identifies remarkably similar losses of
23 H3K9me3 and changes in expression, defining regions where H3K9me3 is secondary to DNA
24 methylation. We show that ZFP57 is the principal methylation-sensitive KZFP recruiting KAP1 and
25 H3K9me3 in ES cells. Finally, like imprints, other unique targets of ZFP57 are enriched for germline-
26 derived DNA methylation including oocyte-specific methylation that is resistant to post-fertilisation
27 epigenetic reprogramming.

28 **Conclusion:** Our analyses suggest the evolution of a rare DNA methylation-sensitive KZFP that is
29 not essential for repeat silencing, but whose primary function is to maintain DNA methylation and
30 repressive histone marks at germline derived imprinting control regions.

31 **Keywords:** DNA methylation, KZFPs, ZFP57, Transposable elements, Embryonic stem cells

32

33 **Main Text**

34 Kruppel-associated (KRAB)-zinc finger proteins (KZFPs) represent one of the largest families of
35 DNA binding proteins. They are represented in most but not all vertebrate species [1–4], with a
36 recent study mapping the target sites of over 200 KZFPs in human HEK293T cells predominantly to
37 transposable elements including endogenous retroviruses (ERVs) [4]. This is consistent with a small
38 number of more focused studies investigating individual KZFPs in the regulation of transposable
39 elements. For example, KZFPs such as ZFP809 [5], ZFP932 and its paralog Gm15446 [6], and
40 ZNF91/93 [7] have each been shown to repress different retrotransposon families in mouse
41 embryonic stem cells (ES cells). Collectively, these and other studies [8,9] suggest that the main
42 function of KZFPs is to regulate transposable elements. The binding of KZFPs to retrotransposons
43 is associated with their transcriptional silencing and is mediated by recruitment of the KAP1 (also
44 known as TRIM28 or TIF1 β) co-repressor complex, which induces the local acquisition of H3K9me3.
45 Members of the co-repressor complex include the histone methyltransferase SETDB1 (also known
46 as ESET), heterochromatin protein 1 (HP1), the histone demethylase LSD1, and NuRD histone
47 deacetylase complex [10,11]. Loss of KAP1 binding leads to the specific loss of H3K9me3 [12].

48 Individual KZFPs have also been noted to bind to unique regions of the mammalian genome [4,13–
49 15]. In particular, a role for ZFP57 in the targeted maintenance of genomic imprints has provided
50 novel insights into functions of this family outside the management of the repeat genome. Genomic
51 imprinting is a process that causes genes to be expressed according to their parental origin.
52 Imprinted genes are regulated by parental origin-specific DNA methylation at imprinting control
53 regions (ICRs), that is acquired at different locations in the male and female germlines (germline
54 differentially methylated regions, gDMRs) and maintained after fertilization during preimplantation
55 epigenetic reprogramming [16]. *In vivo*, ZFP57, with ZFP445, is required to maintain the methylation
56 memory of parental-origin during this critical dynamic epigenetic period. ZFP57 binds to all ICRs in
57 ES cells [15,17–20] with the exception of *Slc38a4*, which appears to be regulated in a different
58 manner [21]. In humans, mutation of ZFP57 has been found in patients with multi-locus imprinting
59 disturbances including transient neonatal diabetes mellitus type 1 (TNDM1) [22,23]. Furthermore, in
60 mice, ZFP57 exerts a maternal-zygotic effect, whereby deletion of both the maternal gene in
61 oocytes and the zygotic copies in early embryos causes severe loss of methylation imprints at
62 multiple imprinted loci, resulting in embryonic lethality. Homozygous deletion of only the zygotic
63 ZFP57 presents a partially penetrant lethal phenotype [15]. Binding of ZFP57 to other unique
64 regions has also been described, including strain-specific interactions conferred by genotype
65 specific polymorphisms in ZFP57 recognition sites [18]. Though correlated with strain-specific
66 transcriptional behavior in some instances [18,24], the functional importance of such interactions at
67 non-imprinted loci *in vivo* are not known.

68 In order to determine the relative importance of ZFP57 binding at different genomic locations, we
69 assessed whether ZFP57 function in ES cells extends beyond the regulation of imprinted regions
70 including at retrotransposons. We found extensive ZFP57 binding at unique germline methylated
71 sites outside imprinted domains, whilst the vast majority of binding was targeted to transposable
72 elements (TEs). Deletion of ZFP57 resulted in loss of KAP1 binding and H3K9me3 at imprinted
73 locations as well as at ~100 other unique ZFP57 targets. In contrast to imprinted domains, this was
74 only modestly correlated with changes in expression of nearby genes suggesting a functionally
75 distinct role for ZFP57 at these regions. With few notable exceptions, TEs maintained H3K9me3
76 supporting the idea that they may be transcriptionally silenced by multiple redundant mechanisms
77 involving other KZFPs in ES cells [4,6,25,26]. This pattern of retained H3K9me3 was also observed
78 in ES cells derived from embryos with maternal-zygotic ZFP57 deletion. Interestingly, the pattern of
79 ZFP57 binding in ES cells essentially mimicked sites where H3K9me3 was lost in DNA
80 methyltransferase (*Dnmt1/Dnmt3a/Dnmt3b*) triple knock out (DNMT TKO) ES cells [26], indicating a
81 primary role for DNA methylation in the establishment of H3K9me3 via ZFP57. Thus, we propose
82 that the primary role of ZFP57 is in maintenance of genomic imprints via its DNA methylation-
83 sensitive binding, and that its interaction with other targets occurs by virtue of their existing DNA
84 methylation status, perhaps providing reinforcement of an already silenced state.

85

86 **Results**

87 **Analysis of blastocyst derived ZFP57 null ES cells**

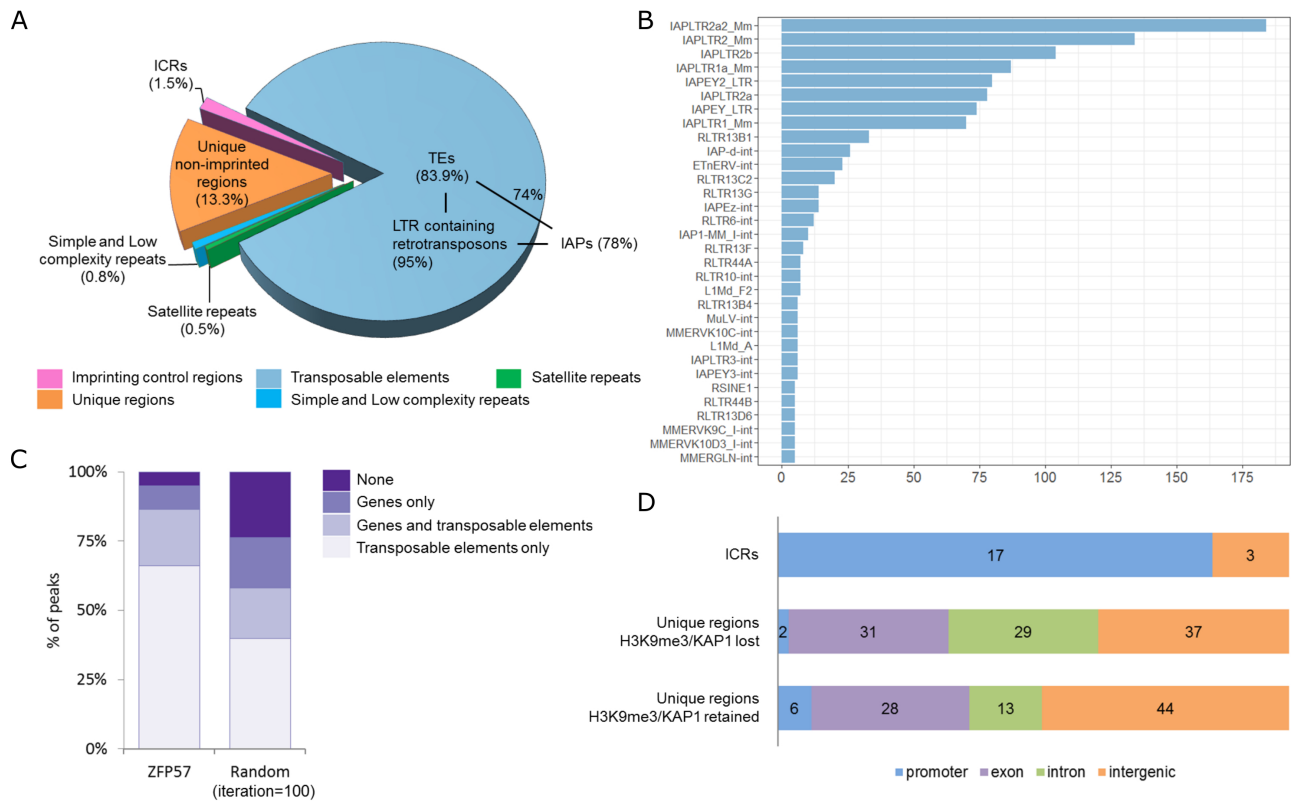
88 To better understand the role(s) played by ZFP57 during preimplantation development we have
89 derived ZFP57 null ES cells directly from C57BL/6J (BL6) blastocyst embryos in ground state
90 pluripotency conditions [27]. ZFP57 homozygous mutant ES cells (ZFP57 KO) were derived from
91 embryos which targeted coding exon 4 and 5 comprising both the KRAB domain and zinc fingers
92 [19]. Genotyping analysis of ES cells showed the expected Mendelian ratios, enabling selection of
93 both wild-type and mutant male lines for further analysis. In addition, we derived two maternal-
94 zygotic ZFP57 deleted (ZFP57 MZ-KO) ES cell lines on mixed C57BL/6J–129/SvS1 (BL6/129)
95 background. These could not be generated on a pure C57BL/6J background since homozygous
96 BL6 mutant females do not survive to term. Absence of ZFP57 protein in mutants was confirmed by
97 western blot analysis on whole cell extracts (Fig. S1A). Quantitative bisulfite pyrosequencing
98 confirmed loss of methylation imprints in all the mutants consistent with previous reports [17,24],
99 with the exception of KvDMR1, where no loss of DNA methylation was observed in these cells (Fig.
100 S1B). These results show for the first time, that loss of imprinting is equivalent in both zygotic and
101 maternal-zygotic ZFP57 mutant ES cells.

102 **Mapping of genome-wide ZFP57 binding sites in ES cells reveals binding events at**
103 **transposable elements in addition to unique non-imprinted genes**

104 We mapped ZFP57 genomic targets by ChIP-seq in WT and ZFP57 KO ES cell lines using an
105 antibody that recognizes endogenous ZFP57. In total, we identified 1423 high-confidence ZFP57
106 peaks, where each peak was independently called in at least two of three WT biological replicates.
107 As expected, we observed strong ZFP57 binding at 20 of the 22 known ICR elements, including
108 binding at previously identified tissue specific imprinted genes *Cdh15* [28], with weaker peaks at the
109 two remaining imprints lying below the peak threshold (*Gpr1* and *Mcts2*). As in our previous report,
110 no binding was detected at the *Slc38a4* DMR [18], in agreement with study demonstrating a role for
111 H3K27me3 in regulating its germline imprinting [21].

112 Using this stringent cut-off, the remainder of the ZFP57 peaks were further characterized according
113 to their relative location at unique regions and at different types of repetitive elements in the mouse
114 genome. We found 13.5% (n=189) targets mapped to non-repetitive regions, a further small subset
115 of peaks 1.3% (n=19) at non-transposon derived repeats (e.g. Simple, low complexity and satellite
116 repeats), whilst the vast majority of the peaks 85.2% (n=1194) targeted transposable elements (Fig.
117 1A). In total, ZFP57 binds 1061 LTR containing retrotransposons of which the majority (n=795) were
118 IAPs, with IAPLTR2a2_Mm representing the largest class (Fig. 1B). In total, ~7-8% of all IAPs
119 present in the mouse genome are bound by ZFP57 in ES cells. This binding to repeats was highly
120 specific since only uniquely aligned reads were used for peak calling (based on paired-end read
121 mapping) (Fig. S2). TE enrichment in the ZFP57-bound subset of repeats was highly significant in
122 comparison to the rest of genome (Fig. 1C, $P < 0.0001$).

123



124

125 **Fig. 1. Genome-wide mapping of ZFP57 binding sites in ES cells.** (A) Distribution of ZFP57 binding sites
126 with respect to unique regions and repetitive elements. (B) Top 32 TE classes bound by ZFP57, ranked by
127 number of ZFP57 peaks. IAPLTR2a2_Mm represents the most commonly targeted TE by ZFP57. (C)
128 Significant enrichment of ZFP57 peaks at TEs relative to random peak permutations, number of iterations
129 =100, binomial $P < 0.0001$. (D) Non-repeat associated peaks bind distinct genomic regions within ICRs and
130 non-imprinted regions.

131 Analysis of non-repeat associated ZFP57 peaks revealed a distinct distribution of imprinted versus
132 non-imprint bound sites with respect to gene features. Whilst maternally methylated ICRs coincide
133 with gene promoters, the majority of non-imprint associated peaks were equally distributed within
134 gene exons, introns and intergenic regions (Fig. 1D). Indeed, very few promoter-bound sites lay
135 outside imprinted regions, but notably included the promoter of the *Dux* gene – a transcription factor
136 involved in zygotic genome activation at the 2 cell stage [29,30]. Our analysis of data from Imbeault
137 et al, revealed that the human DUX4 promoter is targeted by multiple KZFPs including ZFP57 [4],
138 consistent with our observation that H3K9me3 is only partially lost at this locus in ZFP57 mutants.

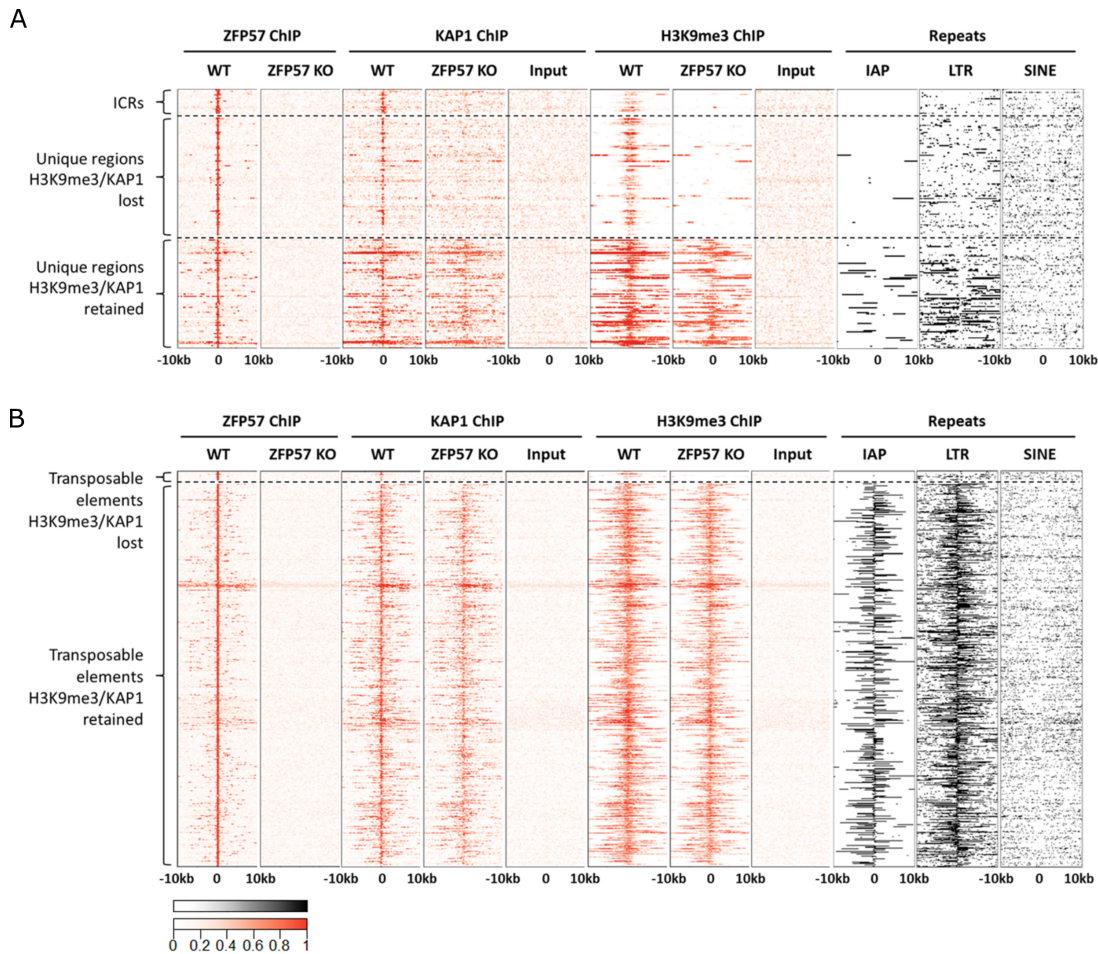
139

140 **Distinct H3K9me3 and KAP1 binding profile at ZFP57 bound unique regions and**
141 **transposable elements**

142 KZFPs are associated with the KAP1 mediated recruitment of SETDB1 and in turn H3K9me3
143 deposition. We therefore examined the presence or absence of KAP1 and H3K9me3 in ZFP57 KO
144 cells by ChIP-seq. Once again, using ICRs as internal controls, we found the expected loss of KAP1
145 binding at almost all ICRs (n=20), of which 17 also exhibited complete loss of H3K9me3 (Fig. 2 and
146 Fig. S3). Interestingly, H3K9me3 was also lost at *KvDMR1* ICR – the only DMR retaining DNA
147 methylation in the KO ES cells (Fig. S1a and Fig. S3). Three ICRs: *Grb10*, *Fkbp6* and *Peg10*
148 exhibited varying degrees of loss of H3K9me3 and KAP1 binding (Fig. S4).

149 We next analyzed the genome-wide distribution of KAP1 and H3K9me3 at different categories of
150 ZFP57 peaks in WT and KO cells. Approximately one half (n=98, 52%) of the unique non-ICR peaks
151 exhibited complete loss of KAP1 and H3K9me3 in ZFP57 mutant ES cells, whilst the rest (n=91,
152 48%) retained KAP1 binding and H3K9me3 (Fig. 2A). Upon further inspection of the H3K9me3
153 retaining group it was revealed that although mapping to unique sequences, they are found in more
154 repeat-dense genomic regions with specific enrichment of LTR-containing retrotransposons ($P <$
155 0.001, unpaired two-tailed t-test) encompassing IAPs (Fig. 2A, right panel). We speculate that KAP1
156 binding (presumably recruited by other KZFPs) at those nearby retrotransposons maintains a
157 generally repressed state of the entire region irrespective of ZFP57 binding.

158



159

160 **Fig. 2. Distinct H3K9me3 and KAP1 binding profile at ZFP57 bound unique regions and transposable**
 161 **elements.** (A) Heat maps of ChIP-seq enrichment signals (red) within ICRs/unique regions and (B)
 162 transposable elements associated binding sites. Enrichment of IAP, LTR and SINE elements are shown as
 163 black-and-white heat maps. Within unique regions, significant enrichment for LTRs nearby H3K9me3 retaining
 164 group compared to H3K9me3 losing group was observed by measuring distance to the nearest LTR from
 165 each peak (unpaired two-tailed t-test, $P < 0.001$).

166 In contrast to the unique ZFP57 target sites, virtually all ZFP57 peaks at transposable elements
 167 (98%; $n=1168$) retained H3K9me3 levels (Fig. 2B). Only 26 (2.2%) TEs showed loss of KAP1 and
 168 H3K9me3 and these were mainly SINEs, non-IAP retroelements or solo IAP-derived LTRs. We thus
 169 conclude that despite widespread binding of ZFP57 to transposable elements, it is not required for
 170 their repression.

171 Finally, we mapped H3K9me3 profiles in ES cells derived from maternal-zygotic deletion of ZFP57
 172 (Fig. S5). Despite the more penetrant phenotype *in vivo* of the maternal zygotic deletion [15], we
 173 observed a nearly identical pattern of H3K9me3 loss/retention over the unique and repeat
 174 associated subsets of peaks in ZFP57 MZ-KO ES cells.

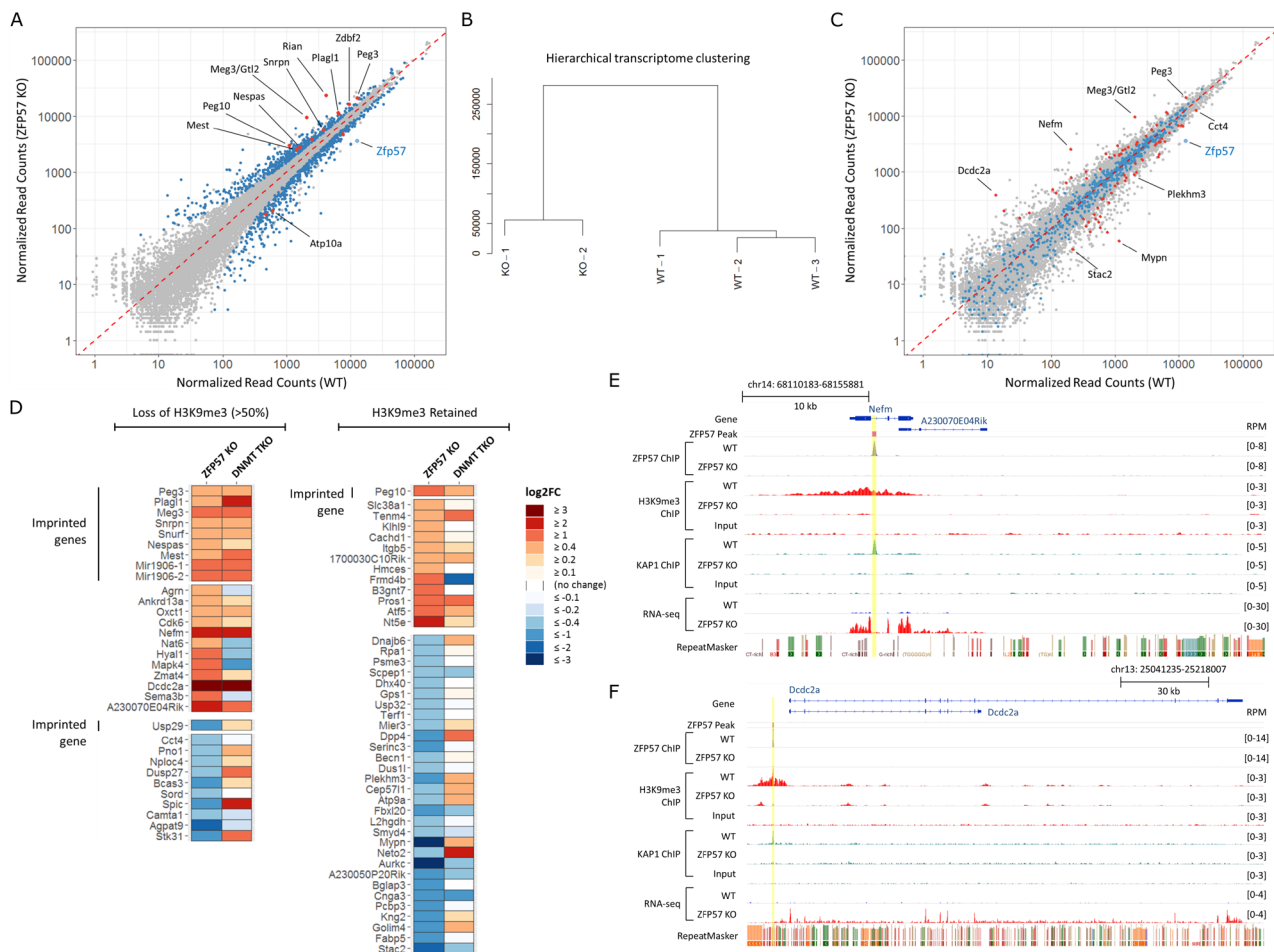
175

176 **Transcriptional profiling identifies few specific non-imprinted ZFP57 target genes**

177 To determine the functional consequences of ZFP57 deletion on the transcriptome, total RNA
 178 sequencing post-ribosomal RNA (rRNA) depletion was performed on these same control and
 179 mutant cell lines.

180 Genome-wide differential expression analysis revealed statistically significant altered expression of
 181 1080 genes in ZFP57 KO cells in comparison to WT, which included many known imprinted genes
 182 in agreement with previously demonstrated roles of ZFP57 in imprint regulation (Fig. 3A).

183 Quantification of all annotated gene transcripts followed by hierarchical clustering analysis indicated
 184 clear segregation of the WT and mutant cell lines (Fig. 3B). In order to determine whether non-
 185 imprint bound ZFP57 regions might regulate expression of nearby genes, we analyzed expression
 186 of all genes in close proximity (< 20 kb) to ZFP57 peaks (n=748, Fig. 3C). We found that only a
 187 small subset (n=75) of differentially expressed genes harbored ZFP57 binding sites or have ZFP57
 188 peaks located nearby (< 20kb). Thus, the majority of differentially expressed genes may not be
 189 direct targets of ZFP57 and instead may represent secondary effects of a perturbed imprinted gene
 190 network.



191

192 **Fig. 3. ZFP57 KO ES cells show perturbed expression of imprinted and non-imprinted genes.** (A)
193 Scatterplot of gene expression in WT and ZFP57 KO ES cells with differentially expressed genes identified by
194 DESeq2 shown in blue, of which the known imprinted genes further highlighted in red. (B) Hierarchical
195 transcriptome clustering analysis showing clear segregation of WT versus KO cells. (C) Scatterplot as in (A),
196 but highlighted all the genes < 20kb of ZFP57 peak, blue = no significant change in expression of associated
197 genes (n=673), red = differentially expressed (n=75). (D) Gene expression differences within the 75 genes,
198 with ZFP57 peaks losing H3K9me3 shown on the left, and those retaining H3K9me3 shown on the right.
199 Expression of ZFP57 KO and DNMT TKO versus their corresponding WT control is shown side by side for
200 comparison. (E) Genome browser screenshots for the two highest upregulated non-imprinted genes *Nefm* and
201 (F) *Dcdc2a*, showing relative location of ZFP57 peak, H3K9me3/KAP1 enrichment and RNA-seq tracks for
202 each gene.

203 We ascertained whether the 75 ZFP57-bound differentially expressed genes were misregulated as
204 a direct consequence of loss of H3K9me3 and/or DNA methylation in ZFP57 KO ES cells by
205 comparing this with their expression levels in DNMT TKO ES cells lacking both maintenance and de
206 novo DNA methyl transferases [26]. These cells are devoid of any detectable 5-methylcytosine
207 (5mC) in the genome, and as ZFP57 binding is DNA methylation dependent, they are unable to
208 target ZFP57 binding. We found that genes upregulated in ZFP57 KO ES cells had a strong
209 tendency to be also upregulated in DNMT TKO cells suggesting these are direct ZFP57 targets (Fig.
210 3D, top). This correlation was strongest amongst imprinted genes. In contrast, no such correlation
211 could be seen in genes that are downregulated in ZFP57 null ES cells (Fig. 3D, bottom) indicating
212 that those are likely to be secondary effects. Amongst the strongest upregulated non-imprinted
213 genes in both mutants were the *Nefm* and *Dcdc2a* genes (Fig. 3E and Fig. 3F). In both cases, loss
214 of ZFP57 led to loss of KAP1 binding, and abolition of a repressive H3K9me3 domain around the
215 gene indicating a primary role for DNA methylation in the recruitment of repressive epigenetic state
216 at these regions via ZFP57.

217 In conclusion, we find a large network of gene deregulation occurring in ZFP57 KO ES cells,
218 however, apart from imprints, only a small proportion of non-imprinted genes are likely to be directly
219 regulated by ZFP57.

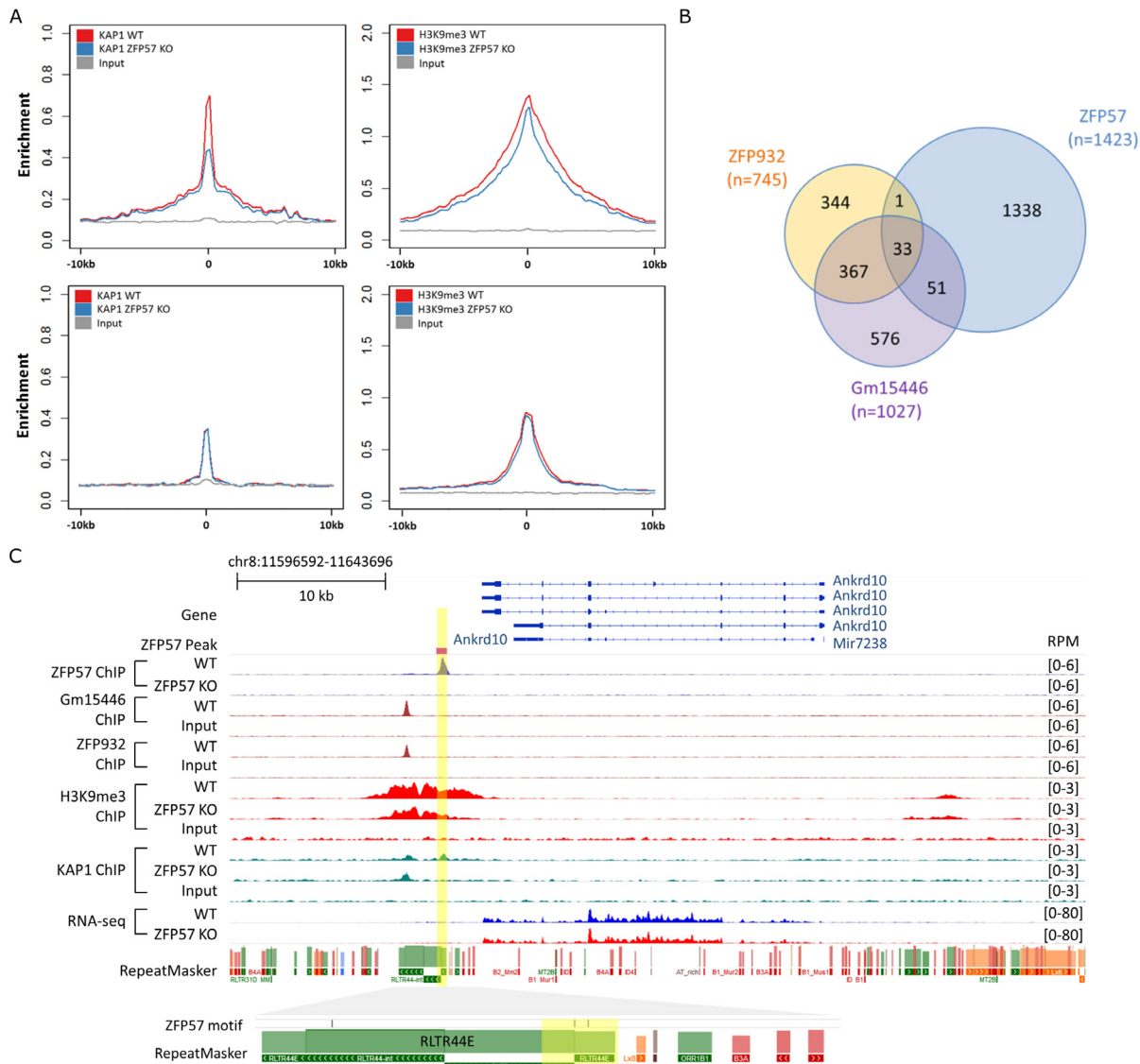
220

221 **ZFP57 at transposable elements**

222 Given the widely accepted role of KZFPs in silencing retroelements, we further explored whether
223 ZFP57 binding to transposable elements is functional or coincidental. The vast majority of ZFP57-
224 bound transposable elements retained H3K9me3 in mutants (Fig. 2B) and remained
225 transcriptionally repressed (Fig. S6). Interestingly, despite the overall retention of H3K9me3
226 enrichment, we observed a reduction of KAP1 signal at ZFP57 bound TEs in the mutants (Fig. 4A),

227 indicating some contribution to the recruitment of KAP1. We hypothesized that the retained
228 repression of retrotransposons in ZFP57 KO ES cells might be mediated by binding of other KZFPs
229 recruiting KAP1 at levels sufficient to maintain H3K9me3. A recent screen for KZFPs that target
230 retrotransposon silencing identified ZFP932 and Gm15446 as partially redundant factors binding to
231 endogenous retroviruses including IAPs [6]. We overlapped these published binding sites with those
232 at ZFP57 and identified a subset (n=85) of targeted transposable elements that are jointly bound by
233 ZFP57 (Fig. 4B). One example of this is shown for the RLTR44E retroelement located ~2kb
234 downstream from the *Ankrd10* gene and harbors adjacently located ZFP57 and ZFP932/Gm15446
235 peaks (Fig. 4C). In ZFP57 null ES cells, KAP1 is specifically lost under the ZFP57 peak, whilst being
236 maintained at the neighboring site of two other KZFPs. Consequently, the region of the repeat
237 maintains overall H3K9me3 levels and neither reactivation of RLTR44E nor *Ankrd10* was observed
238 in ZFP57 mutants. Amongst triply bound transposable elements in general, no reactivation was
239 observed in either the ZFP932/Gm15446 double deletion or ZFP57 KO ES cells (with exception of
240 the IAP retroelement in the vicinity of *Bglap3*), indicating potential for redundant functions of KZFPs
241 (Fig. S7).

242



243

244 **Fig. 4. ZFP57 may contribute to transposon silencing.** a, Reduction of KAP1 ChIP signals in ZFP57 KO
 245 under TE-bound ZFP57 peaks, which leads to very modest reduction in H3K9me3 levels (top), no such
 246 reduction was observed at other KAP1 bound TEs in absence of ZFP57 binding (bottom). b, Venn diagram
 247 showing partially overlapping ZFP57, ZFP932 and Gm15446 peaks. 33 ERVs were found to be triply co-
 248 bound. c, Genome browser screenshot of a triply co-bound RLTR44E retroelement near Ankrd10 gene.
 249 Notably, there's a partial loss of H3K9me3 under ZFP57 peak in ZFP57 KO but not adjacent
 250 ZFP932/Gm15446 peaks, thus maintaining overall silencing of the repeat and unchanged levels of the
 251 proximal gene.

252

253 Intriguingly, ~2% of transposable elements (n=26) bound by ZFP57 did exhibit loss of KAP1 and
 254 H3K9me3 (Fig. 2B). However, apart from two notable exceptions this was not associated with
 255 transcriptional activation of the repeat itself or of the nearby coding gene. In one case, loss of
 256 ZFP57 binding at the intergenic MER20 (a DNA transposon) led to an increase in expression of an

257 unannotated transcript comprising both unique regions and a cluster of transposable elements (Fig.
258 S8). In the other example, the IAP derived LTR showed loss of H3K9me3 and KAP1 binding and
259 this was associated with increased expression of the host coding gene *Mapk4* (Fig. S9). Notably
260 this element comprised the LTR only and not the full length IAP, supporting the general rule that
261 IAPs are not affected by ZFP57 ablation.

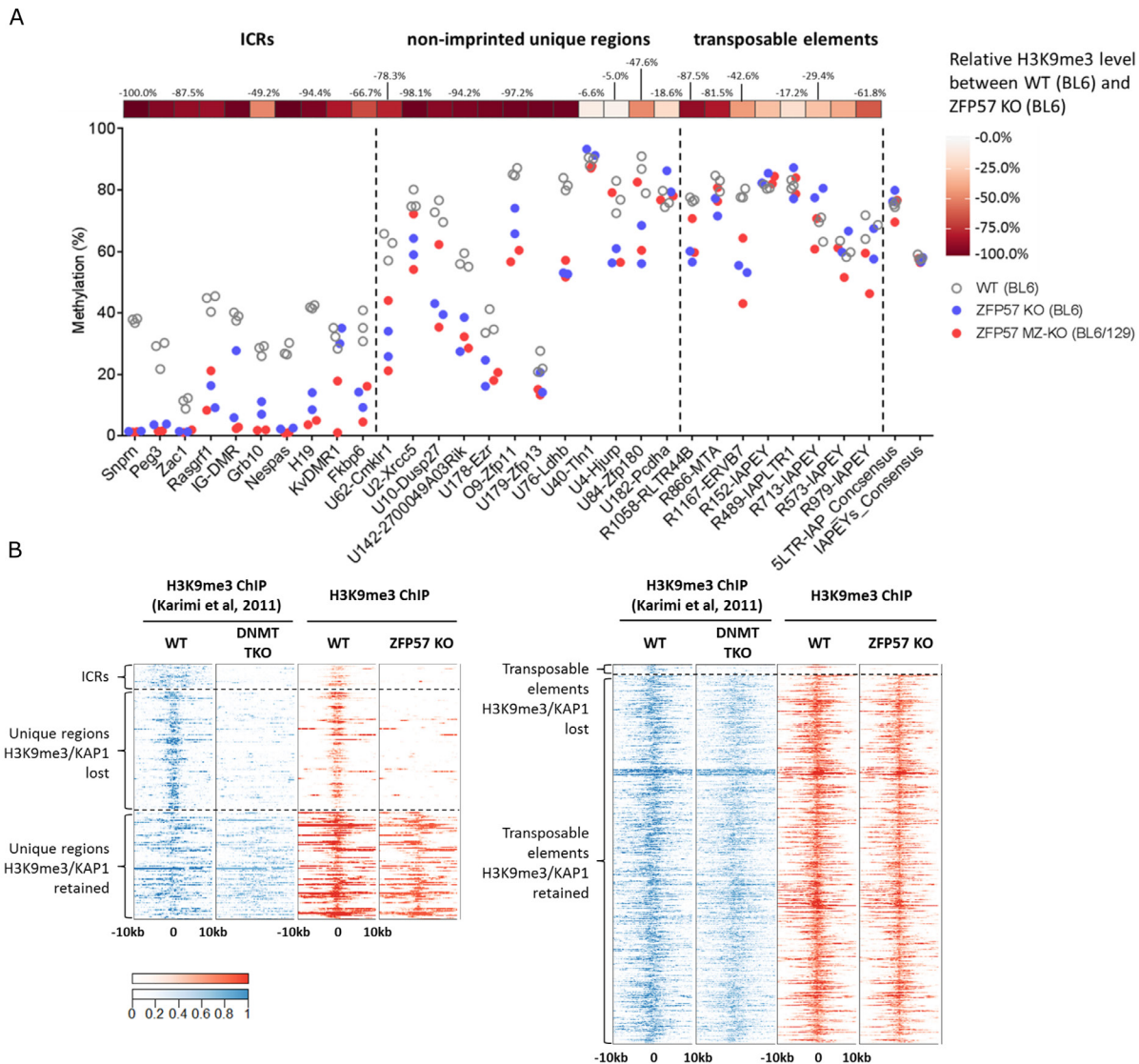
262 Together our data suggest that despite widespread binding of ZFP57 at transposable elements,
263 only a very small subset of them is dependent on this to maintain H3K9me3. This might be partially
264 explained by other KZFPs binding alongside ZFP57 to recruit repressive states to these elements.
265 However, the highly redundant and combinatorial nature of KZFPs binding to transposable elements
266 makes it difficult to ascertain the complexities of these relationships.

267

268 **Relationship between DNA methylation and H3K9me3 at ZFP57 targets**

269 In order to explore the relationship between DNA methylation and H3K9me3 at different types of
270 ZFP57 targets in more detail, we analyzed DNA methylation levels at these regions using
271 quantitative bisulfite pyrosequencing. As expected, we found that loss of ZFP57 and H3K9me3 was
272 associated with loss of DNA methylation at imprints. Regions retaining H3K9me3 (both transposons
273 and unique non-imprinted peaks) remain DNA methylated (Fig. 5A). Interestingly, non-imprinted
274 regions that lost H3K9me3 retained considerable levels of DNA methylation indicating that DNA
275 methylation at these loci was not dependent on H3K9me3.

276



277

278 **Fig. 5. Relationship between DNA methylation and H3K9me3 at ZFP57 binding sites in ES cells.** (A)
 279 Relationship between loss of DNA methylation and loss of H3K9me3 at select ICRs, unique regions and
 280 transposable elements bound by ZFP57. 5' LTR-IAP and IAPEY consensus regions were used as control. (B)
 281 Heat maps of ChIP signals for H3K9me3 in DNMT TKO (blue trace) and ZFP57 KO (red trace) ES cells at
 282 ZFP57 bound unique regions (left) and transposable elements (right).

283

284 Conversely, in order to test if DNA methylation is necessary to confer H3K9me3 at these regions,
 285 we compared the profile of H3K9me3 in ZFP57 KO cells with that of DNA methylation deficient
 286 (DNMT TKO) cells [26]. Strikingly, our analysis identified the pattern of H3K9me3 to be virtually
 287 identical between these two mutants: the repressive mark was lost at ICRs and the exact same
 288 subset of non-imprinted unique regions, whilst maintained over TE-associated ZFP57 peaks (Fig.
 289 5B). Importantly, these data suggest two functions for ZFP57 - one in the maintenance of

290 methylation at imprinted domains, and a second in the methylation-sensitive recruitment of
291 H3K9me3 to some repressed chromatin domains.

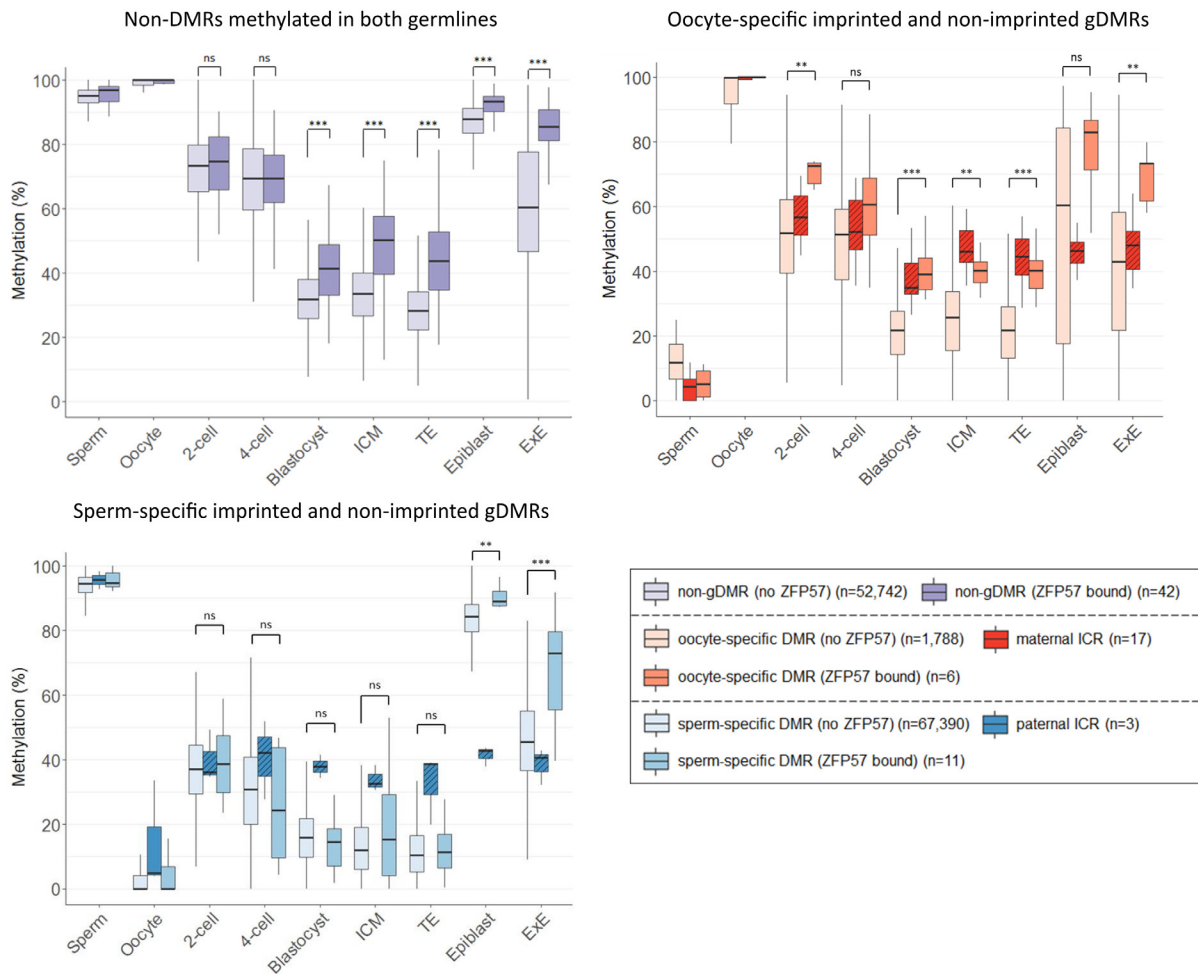
292 Finally, we queried the global extent to which ZFP57 binding sites can explain DNA methylation-
293 dependent H3K9me3 in DNMT TKO cells. In total 15.6% (n=91) of all DNA methylation labile
294 H3K9me3 loci had a strong ZFP57 and KAP1 enrichment signal (Fig. S10). Curiously, the remaining
295 regions (n=492) did not associate with KAP1 indicating that ZFP57 is the main, if not sole, KZFP
296 that recruits repressive histone marks in a DNA methylation-dependent manner in ES cells and that
297 other KAP1-independent processes regulate H3K9me3 at the other sites.

298

299 **ZFP57 maintains germline derived DNA methylation at both imprinted and non-imprinted**
300 **regions during preimplantation development**

301 Imprinting control regions acquire differential DNA methylation in gametes, which is then selectively
302 maintained through preimplantation stages of development. This maintenance has been shown to
303 be ZFP57-dependent *in vivo* for a subset of ICRs [15,19]. We investigated whether non-imprinted
304 unique ZFP57 targets in ES cells are also germline methylated and whether they too are protected
305 from post-fertilization genome-wide erasure of DNA methylation (Fig. 6).

306



307

308 **Fig. 6. ZFP57 maintains DNA methylation at both imprinted and non-imprinted regions during**
 309 **preimplantation development.** DNA methylation level of non-DMRs, oocyte and sperm-specific germline
 310 DMRs bound by ZFP57 (darker coloured) versus those not bound by ZFP57 (light coloured) during
 311 preimplantation development and in E6.5 epiblast and extraembryonic ectoderm [31–33]. Known ICRs are
 312 shown as hatched boxes for comparison. ICM – inner cell mass, TE – trophectoderm, ExE – extraembryonic
 313 ectoderm. ns – not significant, * $P < 0.05$, ** $P < 0.01$, *** $P < 0.001$; Mann-Whitney U Test.

314

315 Analysis of publicly available datasets [31–33] revealed that indeed the majority of unique non-
 316 imprinted targets of ZFP57 where methylation data is available are methylated in both germlines
 317 (n=42), with a few that are either oocyte (n=6) or sperm (n=11) specific gDMRs. We analysed the
 318 DNA methylation dynamics at these regions throughout pre-implantation development and found
 319 that ZFP57 binding conferred significant protection against post-fertilization demethylation in all
 320 oocyte methylated regions regardless whether they are gDMR or not (Fig. 6). Interestingly, sperm-
 321 specific methylated regions with exception of the three known paternal germline imprints are not
 322 protected from DNA methylation reprogramming despite being ZFP57 bound in our ChIP-seq data.
 323 This hints at potentially distinct mechanisms of maintaining germline-derived DNA methylation on

324 the two parental chromosomes by ZFP57. Oocyte-specific gDMRs bound by ZFP57 resolved their
325 DMR status by acquiring DNA methylation in the post-implantation epiblast, resembling patterns that
326 have been previously reported for placenta-specific imprinted and transient maternal gDMRs
327 [28,33–35]. Though numbers are low, sequence composition analysis revealed that non-imprinted
328 paternal DMRs had a lower CpG density compared to the other groups with the maternal ICRs
329 having the highest CpG percentages (Figure S11).

330 Taken together, we conclude that ZFP57 can protect against post-fertilization epigenetic
331 reprogramming at sequences methylated in either or both germlines, and such protection may be
332 associated with local CpG density.

333

334 Discussion

335 In the present study, we demonstrate that in ES cells ZFP57 binds not only to ICRs, but also to non-
336 imprinted unique regions and transposable elements; in particular, to IAPs. We have performed a
337 detailed epigenetic and transcriptomic analysis of ZFP57 mutant ES cells allowing us to ascertain
338 the relative functional roles played by ZFP57 within different genomic locations. We have
339 determined the hierarchical relationship between DNA methylation and H3K9me3 at ZFP57-bound
340 regions, and assessed whether ZFP57 maintains DNA methylation at non-imprinted loci during post-
341 fertilization epigenetic reprogramming.

342 We have identified a subset of unique non-imprinted genomic regions, which depend on DNA
343 methylation and ZFP57 binding for the recruitment of KAP1 and H3K9me3. Only a small proportion
344 of these were associated with significant changes in gene expression in ZFP57 mutants. A striking
345 difference between ICRs and non-imprinted unique ZFP57-bound regions is that the former are
346 predominantly found at promoters, but the latter bind exonic, intronic and intergenic regions. A
347 subset of ZFP57 peaks mapped to the 3' exons of several protein coding genes (n=16) including
348 other Zn-finger transcription factors such as *Zfp13*, *Zfp180* and *Zfp629*. These genes are expressed
349 in WT ES cells and their expression remained unchanged in mutant ES cells despite loss of KAP1
350 and H3K9me3 over the 3' end of these genes. Consistent with this, it has been postulated that 3'
351 end H3K9me3 recruitment may promote genomic stability and prevent recombination between
352 homologous Zn-finger proteins rather than directly regulate their expression [36,37].

353 DNA methylation and H3K9me3 generally co-localize at repressed genomic regions. However, it is
354 not clear where DNA methylation is the driver for the recruitment of H3K9me3 or where it might
355 occur as a secondary consequence of H3K9me3. Studies to investigate this 'cause or consequence'
356 relationship are confounded by the lethality of cells harboring mutations in the H3K9me3 machinery

357 [12,38–40]. Karimi and colleagues have suggested that DNA methylation and H3K9me3 serve to
358 repress distinct sets of genes as well as some classes of retroelements and showed that only a
359 small subset of regions lose their H3K9me3 in DNA methylation deficient (DNMT TKO) ES cells [26].
360 Comparison of the pattern of H3K9me3 loss in DNMT TKO cells with that in ZFP57 KO cells
361 revealed remarkable similarity. The comparison of H3K9me3 in DNMT TKO and ZFP57KO has
362 therefore identified regions where the presence of H3K9me3 is dependent on DNA methylation and
363 showed that it is ZFP57 bound to methylated DNA that is responsible for the H3K9me3 recruitment.
364 The similarity of the transcriptomes in these two mutant cell types is consistent with this and
365 identifies a key role for ZFP57 in the regulation of transcriptional repression of methylated targets in
366 ES cells. Furthermore, ZFP57 binding sites explain a significant proportion of these DNA-
367 methylation dependent H3K9me3 modified regions, including almost all that are KAP1 dependent.
368 This strongly suggests that ZFP57 is the major KZFP that binds DNA in a methylcytosine-dependent
369 manner in mouse ES cells.

370 Recently, we showed that another KZFP member, ZFP445 also binds the methylated allele at
371 imprinted gDMRs and *in vivo* contributes to maintenance of DNA methylation at a subset of ICRs
372 along with ZFP57 [20]. However, data presented here suggests that at least in context of mouse
373 embryonic stem cells, ZFP57 is both necessary and sufficient to recruit KAP1 and maintain
374 H3K9me3/DNA methylation at imprints. Furthermore, our analysis of ZFP445 binding sites (data not
375 shown) revealed very little overlap with ZFP57 outside of imprinted regions with TE-binding being a
376 unique feature of ZFP57.

377 While complete loss of KAP1 and H3K9me3 was observed at ICRs and over half of ZFP57 peaks at
378 unique non-imprinted regions, we found only ~2% of repeat-associated ZFP57 peaks exhibited
379 complete loss of these marks. Our data support the hypothesis that in mammalian ES cells,
380 retroviral silencing is mediated by multiple factors acting in redundant manner. Indeed, we identified
381 extensive overlaps with two other KZFPs (Zfp932 and Gm15446) previously demonstrated to recruit
382 KAP1/H3K9me3 repressive marks to ERVs including IAPs [6]. In this context it is interesting to
383 consider the DNA methylation-sensitive nature of ZFP57 binding [19,41]. This property makes it an
384 unlikely candidate KZFP for the initiation of silencing at the integration site of ERV retro-
385 transposons since it would require DNA methylation to be established first in order for binding to
386 occur. Rather it may contribute to silencing initiated by other KZFPs such as Zfp809 binding to
387 invariable PBS-regions of IAPs [5,9]. Recent studies have suggested that LTR regions have the
388 potential to function as enhancer and/or alternative promoter elements and can be co-opted by the
389 host genome in regulation of its own gene expression [42–45]. The ability of a KZFP to target
390 repressive chromatin states in a methylation-sensitive manner could provide an additional layer of
391 modulation at such loci. However, we also cannot rule out the possibility that ZFP57 binding at

392 these elements is a functionally irrelevant secondary consequence of DNA methylation occurring at
393 already H3K9me3-repressed LTRs that contain the rather common ZFP57 hexanucleotide binding
394 motif.

395 We can now speculate about the function and evolution of ZFP57 in the genome. Indeed, we have
396 shown that ZFP57 mutation does not itself influence the silencing of endogenous retroviral
397 sequences but rather conveys DNA methylation protection to both imprinted and non-imprinted
398 unique CpG rich regions methylated in either or both germlines. Such events may result in the
399 altered dosage of nearby genes, which can then be selected for (e.g. in the case of growth
400 regulating genes) and indeed re-enforced by acquiring extra ZFP57 motifs. Indeed, the majority of
401 known imprinted ICRs contain an unusually high number of ZFP57 motifs within otherwise highly
402 CpG-rich regions setting them apart from other CGIs in the genome. The function, if any, of non-
403 imprinted unique ZFP57 bound regions, which apparently have moderate CpG density and one or
404 two motif instances per peak remains to be determined. We therefore propose that ZFP57 evolved
405 from ancestral KZFPs originally acting to manage retrotransposons, but now functions primarily not
406 to silence these repetitive sequences but rather to control genomic imprinting. This is consistent with
407 the finding that ZFP57 also contributes to the regulation of imprinting in humans [23], a species that
408 lacks the CpG rich IAP retrotransposon sequences to which ZFP57 binds in the mouse.

409

410 **Data availability**

411 All raw and processed data for ChIP-seq and RNA-seq have been submitted to Gene Expression
412 Omnibus (GEO) database under accession number GSE123942.

413

414 **Acknowledgements**

415 This work was funded by grants from the BBSRC (BB/G020930/1) and Wellcome Trust (WT095606) to
416 AFS.

417

418 **Authors' contributions**

419 RS and ACF-S designed the study and conceived the experiments. R.S. and N.T. performed the
420 experiments. H.S. analyzed the data, performed statistical analysis and prepared the figures. A.K.
421 assisted in analysis of repeat data. M.L. provided DNMT TKO data and advised on analysis and
422 data interpretation. H.S., R.S. and A.C.F.-S. interpreted data and wrote the manuscript. M.H. and
423 A.C.F.-S. provided supervision.

424

425

426 **Competing Financial Interest**

427 The authors declare that they have no competing interests.

428

429 **Supplementary Materials**

430 Materials and Methods

431 Fig. S1-S11

432

433 References

- 434 1. Urrutia R. KRAB-containing zinc-finger repressor proteins. *Genome Biol.* 2003;4:231.
- 435 2. Huntley S, Baggott DM, Hamilton AT, Tran-Gyamfi M, Yang S, Kim J, et al. A comprehensive
436 catalog of human KRAB-associated zinc finger genes: Insights into the evolutionary history of
437 a large family of transcriptional repressors. *Genome Res.* 2006;16:669–77.
- 438 3. Emerson RO, Thomas JH. Adaptive evolution in zinc finger transcription factors. *PLoS Genet.*
439 2009;5:e1000325.
- 440 4. Imbeault M, Helleboid P-Y, Trono D. KRAB zinc-finger proteins contribute to the evolution of
441 gene regulatory networks. *Nature.* 2017;543:550–4.
- 442 5. Wolf G, Yang P, Füchtbauer AC, Füchtbauer E-M, Silva AM, Park C, et al. The KRAB zinc
443 finger protein ZFP809 is required to initiate epigenetic silencing of endogenous retroviruses.
444 *Genes Dev.* 2015;29:538–54.
- 445 6. Ecco G, Cassano M, Kauzlaric A, Duc J, Coluccio A, Offner S, et al. Transposable Elements
446 and Their KRAB-ZFP Controllers Regulate Gene Expression in Adult Tissues. *Dev Cell.*
447 2016;36:611–23.
- 448 7. Jacobs FMJ, Greenberg D, Nguyen N, Haeussler M, Ewing AD, Katzman S, et al. An
449 evolutionary arms race between KRAB zinc-finger genes ZNF91/93 and SVA/L1
450 retrotransposons. *Nature.* 2014;516:242–5.
- 451 8. Najafabadi HS, Mnaimneh S, Schmitges FW, Garton M, Lam KN, Yang A, et al. C2H2 zinc
452 finger proteins greatly expand the human regulatory lexicon. *Nat Biotechnol.* 2015;advance
453 on:555–62.
- 454 9. Thomas JH, Schneider S. Coevolution of retroelements and tandem zinc finger genes.
455 *Genome Res.* 2011;21:1800–12.
- 456 10. Sripathy SP, Stevens J, Schultz DC. The KAP1 corepressor functions to coordinate the
457 assembly of de novo HP1-demarcated microenvironments of heterochromatin required for
458 KRAB zinc finger protein-mediated transcriptional repression. *Mol Cell Biol.* 2006;26:8623–38.
- 459 11. Macfarlan TS, Gifford WD, Agarwal S, Driscoll S, Lettieri K, Wang J, et al. Endogenous
460 retroviruses and neighboring genes are coordinately repressed by LSD1/KDM1A. *Genes Dev.*
461 2011;25:594–607.
- 462 12. Rowe HM, Jakobsson J, Mesnard D, Rougemont J, Reynard S, Aktas T, et al. KAP1 controls
463 endogenous retroviruses in embryonic stem cells. *Nature.* 2010;463:237–40.
- 464 13. Fietze S, Lan X, Jin VX, Farnham PJ. Genomic targets of the KRAB and SCAN domain-
465 containing zinc finger protein 263. *J Biol Chem.* 2010;285:1393–403.
- 466 14. Yang P, Wang Y, Hoang D, Tinkham M, Patel A, Sun M, et al. A placental growth factor is
467 silenced in mouse embryos by the zinc finger protein ZFP568. *Science.* 2017;356:757–9.
- 468 15. Li X, Ito M, Zhou F, Youngson N, Zuo X, Leder P, et al. A maternal-zygotic effect gene, *Zfp57*,
469 maintains both maternal and paternal imprints. *Dev Cell.* 2008;15:547–57.
- 470 16. Bartolomei MS, Ferguson-Smith AC. Mammalian genomic imprinting. *Cold Spring Harb*
471 *Perspect Biol.* 2011;3:1–17.
- 472 17. Quenneville S, Verde G, Corsinotti A, Kapopoulou A, Jakobsson J, Offner S, et al. In
473 embryonic stem cells, ZFP57/KAP1 recognize a methylated hexanucleotide to affect

- 474 chromatin and DNA methylation of imprinting control regions. *Mol Cell*. 2011;44:361–72.
- 475 18. Strogantsev R, Krueger F, Yamazawa K, Shi H, Gould P, Goldman-Roberts M, et al. Allele-
476 specific binding of ZFP57 in the epigenetic regulation of imprinted and non-imprinted
477 monoallelic expression. *Genome Biol*. 2015;16:112.
- 478 19. Takahashi N, Gray D, Strogantsev R, Noon A, Delahaye C, Skarnes WC, et al. ZFP57 and
479 the Targeted Maintenance of Postfertilization Genomic Imprints. *Cold Spring Harb Symp*
480 *Quant Biol*. 2015;80:177–87.
- 481 20. Takahashi N, Coluccio A, Thorball CW, Planet E, Shi H, Offner S, et al. ZNF445 is a primary
482 regulator of genomic imprinting. *Genes Dev*. 2019;33:49–54.
- 483 21. Inoue A, Jiang L, Lu F, Suzuki T, Zhang Y. Maternal H3K27me3 controls DNA methylation-
484 independent imprinting. *Nature*. 2017;547:419–24.
- 485 22. Boonen SE, Mackay DJG, Hahnemann JMD, Docherty L, Grønsvov K, Lehmann A, et al.
486 Transient neonatal diabetes, ZFP57, and hypomethylation of multiple imprinted loci: a
487 detailed follow-up. *Diabetes Care*. 2013;36:505–12.
- 488 23. Mackay DJG, Callaway JL a, Marks SM, White HE, Acerini CL, Boonen SE, et al.
489 Hypomethylation of multiple imprinted loci in individuals with transient neonatal diabetes is
490 associated with mutations in ZFP57. *Nat Genet*. 2008;40:949–51.
- 491 24. Riso V, Cammisa M, Kukreja H, Anvar Z, Verde G, Sparago A, et al. ZFP57 maintains the
492 parent-of-origin-specific expression of the imprinted genes and differentially affects non-
493 imprinted targets in mouse embryonic stem cells. *Nucleic Acids Res*. 2016;44:8165–78.
- 494 25. Berrens R V., Andrews S, Spensberger D, Santos F, Dean W, Gould P, et al. An endosRNA-
495 Based Repression Mechanism Counteracts Transposon Activation during Global DNA
496 Demethylation in Embryonic Stem Cells. *Cell Stem Cell*. 2017;21:694–703.e7.
- 497 26. Karimi MM, Goyal P, Maksakova IA, Bilenky M, Leung D, Tang JX, et al. DNA methylation
498 and SETDB1/H3K9me3 regulate predominantly distinct sets of genes, retroelements, and
499 chimeric transcripts in mESCs. *Cell Stem Cell*. 2011;8:676–87.
- 500 27. Nichols J, Jones K. Derivation of Mouse Embryonic Stem (ES) Cell Lines Using Small-
501 Molecule Inhibitors of Erk and Gsk3 Signaling (2i). *Cold Spring Harb Protoc*.
502 2017;2017:pdb.prot094086.
- 503 28. Proudhon C, Duffié R, Ajjan S, Cowley M, Iranzo J, Carbajosa G, et al. Protection against De
504 Novo Methylation Is Instrumental in Maintaining Parent-of-Origin Methylation Inherited from
505 the Gametes. *Mol Cell*. 2012;47:909–20.
- 506 29. Hendrickson PG, Doráis J a, Grow EJ, Whiddon JL, Lim J-W, Wike CL, et al. Conserved
507 roles of mouse DUX and human DUX4 in activating cleavage-stage genes and
508 MERVL/HERVL retrotransposons. *Nat Genet*. 2017;49:925–34.
- 509 30. Iaco A De, Planet E, Coluccio A, Verp S, Duc J, Trono D. Europe PMC Funders Group
510 Europe PMC Funders Author Manuscripts A family of double-homeodomain transcription
511 factors regulates zygotic genome activation in placental mammals. 2017;49:941–5.
- 512 31. Wang L, Zhang J, Duan J, Gao X, Zhu W, Lu X, et al. Programming and inheritance of
513 parental DNA methylomes in mammals. *Cell*. 2014;157:979–91.
- 514 32. Smith ZD, Shi J, Gu H, Donaghey J, Clement K, Cacchiarelli D, et al. Epigenetic restriction of
515 extraembryonic lineages mirrors the somatic transition to cancer. *Nature*. 2017;549:543–7.

- 516 33. Kobayashi H, Sakurai T, Imai M, Takahashi N, Fukuda A, Yayoi O, et al. Contribution of
517 intragenic DNA methylation in mouse gametic DNA methylomes to establish oocyte-specific
518 heritable marks. *PLoS Genet.* 2012;8:e1002440.
- 519 34. Smallwood SA, Tomizawa S-I, Krueger F, Ruf N, Carli N, Segonds-Pichon A, et al. Dynamic
520 CpG island methylation landscape in oocytes and preimplantation embryos. *Nat Genet.*
521 2011;43:811–4.
- 522 35. Stewart KR, Veselovska L, Kelsey G. Establishment and functions of DNA methylation in the
523 germline. *Epigenomics.* 2016;8:1399–413.
- 524 36. Blahnik KR, Dou L, Echipare L, Iyengar S, O'Geen H, Sanchez E, et al. Characterization of
525 the contradictory chromatin signatures at the 3' exons of zinc finger genes. *PLoS One.*
526 2011;6:e17121.
- 527 37. Valle-García D, Qadeer ZA, McHugh DS, Ghiraldini FG, Chowdhury AH, Hasson D, et al.
528 ATRX binds to atypical chromatin domains at the 3' exons of zinc finger genes to preserve
529 H3K9me3 enrichment. *Epigenetics.* 2016;11:398–414.
- 530 38. Dodge JE, Kang Y, Beppu H, Lei H. Histone H3-K9 Methyltransferase ESET Is Essential for
531 Early Development. *Mol Cell Biol.* 2004;24:2478–86.
- 533 39. Messerschmidt DM, de Vries W, Ito M, Solter D, Ferguson-Smith A, Knowles BB. Trim28 is
534 required for epigenetic stability during mouse oocyte to embryo transition. *Science.*
535 2012;335:1499–502.
- 536 40. Lehnertz B, Ueda Y, Derijck AAHA, Braunschweig U, Perez-Burgos L, Kubicek S, et al.
537 Suv39h-mediated histone H3 lysine 9 methylation directs DNA methylation to major satellite
538 repeats at pericentric heterochromatin. *Curr Biol.* 2003;13:1192–200.
- 539 41. Liu Y, Olanrewaju YO, Zhang X, Cheng X. DNA recognition of 5-carboxylcytosine by a Zfp57
540 mutant at an atomic resolution of 0.97 Å. *Biochemistry.* 2013;52:9310–7.
- 541 42. Friedli M, Trono D. The developmental control of transposable elements and the evolution of
542 higher species. *Annu Rev Cell Dev Biol.* 2015;31:429–51.
- 543 43. Chuong EB, Rumi M a K, Soares MJ, Baker JC. Endogenous retroviruses function as
544 species-specific enhancer elements in the placenta. *Nat Genet.* 2013;45:325–9.
- 545 44. Rowe HM, Kapopoulou A, Corsinotti A, Fasching L, Macfarlan TS, Tarabay Y, et al. TRIM28
546 repression of retrotransposon-based enhancers is necessary to preserve transcriptional
547 dynamics in embryonic stem cells. *Genome Res.* 2013;23:452–61.
- 548 45. Thompson PJ, Macfarlan TS, Lorincz MC. Long Terminal Repeats: From Parasitic Elements
549 to Building Blocks of the Transcriptional Regulatory Repertoire. *Mol Cell.* 2016;62:766–76.

550